

## Emission of an Upper-Hybrid-Wave Soliton from an Ion Wave in a Beam-Plasma System

Ichiro Mori

*Technical College of Tokushima University, Minami-Josanjima, 770 Tokushima, Japan*

and

Kaoru Ohya

*Faculty of Engineering, Tokushima University, Minami-Josanjima, 770 Tokushima, Japan*

(Received 25 November 1986)

A new phenomenon that an ion wave emits an upper-hybrid-wave soliton was observed in a beam-plasma system. Observations were performed by the previously developed time-of-flight method. The necessary phase condition between the ion wave and the upper hybrid soliton was recognized and the growth rate of the upper hybrid wave was obtained experimentally.

PACS numbers: 52.40.Db, 52.35.Hr, 52.35.Sb, 52.40.Mj

Several recent theoretical works<sup>1-5</sup> predict that an ion wave will also emit an electrostatic high-frequency wave. This report will discuss a mechanism with regard to generation of the electrostatic wave, especially an upper hybrid soliton.<sup>6</sup>

A feature of this electrostatic wave is in a radiation spectrum where the wavelength of these induced processes belong to the microwave and the radio wave range. We can apply, therefore, our recently developed "new method" to detect the high-frequency wave packets.<sup>7</sup> A schematic drawing of the experimental apparatus is shown in Fig. 1.

The plasma region in which the beam-plasma interaction occurs is 16 cm in diam and 40 cm in length and a mirror magnetic field of 100 G is applied in the center position with a mirror ratio of 1.4. The electron gun region is evacuated to  $10^{-6}$  Torr, while the plasma region is fed with argon gas from  $10^{-4}$  to  $10^{-3}$  Torr. The beam parameter is 2 keV–20 mA.

At the end of the plasma region, a beam collector is

set up, which is a water-cooled copper disk with a diameter of 14 cm. The disk is grounded through a 50- $\Omega$  resistor, for current measurement. A blocking capacitor is connected to one end of the resistor. The signal passes through the blocking capacitor and a high-pass filter with a cutoff frequency of 30 MHz. Thus, the dc component (such as an ambipolar potential) and a lower-frequency component of electron beam current (such as an ion wave) are rejected by the filter. However, a high-frequency component of the electron current, for instance 400 MHz for the carrier of a wave packet, passes through and is detected by a diode whose frequency characteristic is flattened up to 800 MHz. The detected signal is amplified and is observed finally by an oscilloscope. The plasma electron temperature is 3 eV at a pressure of  $5 \times 10^{-4}$  Torr, measured in the center by a radial probe. Plasma density is controllable up to  $10^{11}$  cm<sup>-3</sup>, but normally a density between  $10^8$  and  $10^9$  cm<sup>-3</sup> is used.

In order to detect the plasma and excited field, three probes are inserted in the plasma region which are used as antennae. A pickup signal obtained by the antenna is sent to an attenuator. Then the signal passes through a blocking capacitor of 0.18  $\mu$ F and a high-pass filter (HPF). The signal drives a constant-fraction discriminator (CFD). The CFD provides an enhanced timing resolution due to elimination of the leading-edge errors of triggering and also provides a transistor-transistor logic output into a 50- $\Omega$  load. The time difference between the leading edge of the rectangular signals from each CFD is converted into a pulse height with a time-to-amplitude converter (TAC). The TAC generates a rectangular analog output pulse whose peak amplitude is linearly proportional to the time interval between a start and a subsequent stop input. Both are derived from the CFD. A multichannel analyzer measures the peak amplitudes of output pulses from the TAC and gives a two-dimensional graphic formula.

Ordinarily, nonlinear effects become important when

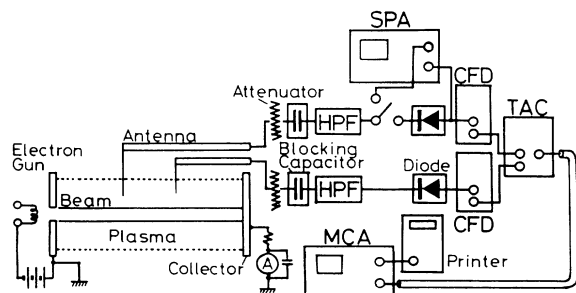


FIG. 1. Schematic drawing of the experimental apparatus. A pickup signal from an antenna passes through a high-pass filter (HPF) and drives a constant-fraction discriminator (CFD). The time difference between the signals from each CFD is converted into a pulse height with a time-to-amplitude converter (TAC). Then the pulse height is analyzed by a multichannel analyzer (MCA).

the wave-energy density,  $W$ , becomes much larger than at thermal equilibrium [ $W \gg nkT(n\lambda_d^3)^{-1}$ ], but is still much smaller than the thermal-energy density ( $W \ll kT$ ), where  $n$ ,  $T$ , and  $\lambda_d$  are the electron density, temperature, and the Debye length, respectively.<sup>8</sup> We measured the absolute wave field inside the plasma as in previous studies where the measurement was performed by using the Hewlett-Packard model 8554L-8552B spectrum analyzer system. The probe sustained damage from bombardment of the beam electrons in the region  $r < 0.9$  cm, so data in this region were not obtained. An extrapolation, however, gives a value of  $E = 15$  V/cm on the axis ( $r = 0$  cm).<sup>9</sup> Using the parameters in the beam-plasma system, we can examine the above-mentioned condition and obtain the following result:  $W/nkT(n\lambda_d^3)^{-1} \approx 10^3$ . This value satisfies the above-mentioned condition as a measure of turbulence.

Now, in our beam-plasma system, one can adjust a focusing coil current and focus the electron beam into one point in the plasma. The diameter of the point is about 8 mm. Then a large-amplitude ion wave, which is considered to be a continuous shock wave, arises from the point. The mean free path of an electron-neutral collision,  $l$ , is estimated as a few meters under our experimental conditions while the width of the ion wave,  $d$ , is a few centimeters so that a condition  $l \gg d$  is fulfilled which satisfies the requirements for a collisionless shock wave. Figure 2(a) shows a profile of an ion wave obtained by the time-of-flight method. The results of a multiexposure photograph on the upper hybrid wave are presented in Fig. 2(b), where the sweep-time scale of 5  $\mu\text{s}/\text{div}$  and a 2.75- $\mu\text{s}$ -delayed sweep are utilized.

The shock wave is expected to be satisfied by the Korteweg-de Vries (KdV) equation with a term of attenuation where the term describes a mechanism of dissipation. The mechanism of the dissipation will be the nonlinear Landau damping which corresponds to the emission of an upper hybrid soliton.

Experimental evidence that the curve in Fig. 2(a) satisfies the KdV equation was obtained by measuring the distance between a peak and an adjacent peak, which is proportional to the inverse of the wave number without considering the damping, and by counting the channel number of each peak where the channel number is inversely proportional to a group velocity. Thus, the experimental evidence that the wave satisfies the KdV equation was obtained by testing the wavelength to see whether it agrees with a theoretical dispersion relation.

By using the generalized Boussinesq equation and a continuous equation, we can derive the following equation<sup>10</sup>:

$$\partial v / \partial t + \{c_0 + (\gamma + 1)v/2\}(\partial v / \partial x) + \beta(\partial^3 v / \partial x^3) = 0, \quad (1)$$

where  $c_0$ ,  $\beta$ , and  $\gamma$  are sound velocity, dispersion parameter, and effective adiabatic index, respectively. If we

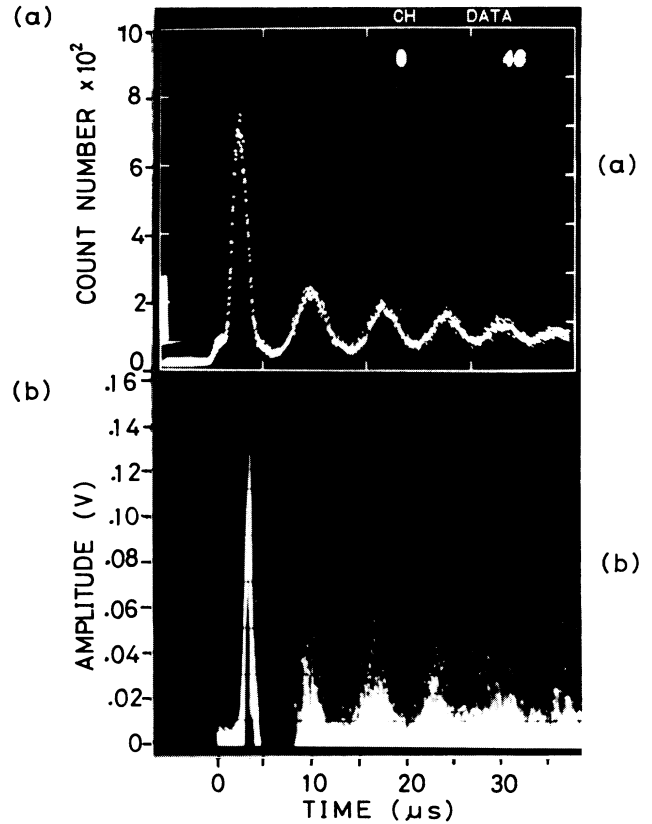


FIG. 2. (a) Profile of the ion shock wave obtained by the time-of-flight method. (b) High-frequency component of a collector current. The figure shows a high-frequency emission from the ion shock wave which is presented in (a).

consider the coordinate moving with the sound velocity and use new variables

$$x' = x - c_0 t, \quad t' = t, \quad u = (\gamma + 1)v/2, \quad (2)$$

then Eq. (1) becomes the KdV equation

$$\partial u / \partial t + u(\partial u / \partial x) + \beta(\partial^3 u / \partial x^3) = 0, \quad (3)$$

where we omit the primes for simplicity. Now we define  $\alpha$  as

$$\alpha = c_0 + (\gamma + 1)v/2. \quad (4)$$

If we suppose that  $\alpha$  is constant, then a linearized dispersion relation can be obtained from Eq. (1) as

$$\omega = \alpha k - \beta k^3. \quad (5)$$

By differentiating Eq. (5) with  $k$ , we get finally the following expression:

$$\partial \omega / \partial k = \alpha - 3\beta k^2. \quad (6)$$

In the experiment, the group velocity  $\partial \omega / \partial k$  is measurable by the time-of-flight method, while  $k$  is obtained from the distance between adjacent peaks of the curve.

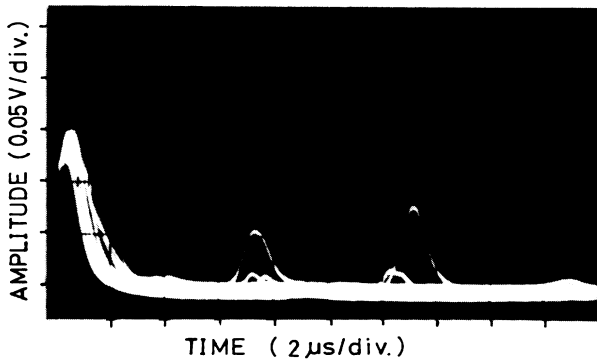


FIG. 3. Detected signal of high-frequency component in the collector current. The signal shows an envelope since it is detected by a diode.

If we neglect the effect of dispersion, the group velocity equals  $c_0$ . However,  $\alpha$  is not a constant actually and its value is different in different parts of the wave. The experimental result obeys the relation

$$\frac{\alpha}{c_0} = \frac{\text{channel number of peak No. 1}}{\text{channel number of each part}} \quad (7)$$

This relation corresponds to Eq. (4).

Figure 3 shows a detected signal of the high-frequency component in the beam current derived from one end of the 50- $\Omega$  resistor which is connected to a beam collector. The signal is observed by an oscilloscope. The horizontal axis shows the sweep time of the oscilloscope on the scale of 2  $\mu\text{s}/\text{div}$ , and multitrace mode was used. The vertical axis shows the amplitude measured on the scale of 0.05 V/div. From the figure, it is seen that an upper hybrid wave was emitted to satisfy the phase condition which was expected from the theory<sup>3</sup> and that the efficiency of the emission is higher when the amplitude of the ion wave is large. In contrast, emission becomes uncertain when the amplitude is small.

Thus, upper hybrid solitons having a center carrier frequency of 399 MHz are detected only in the presence of ion waves when the wave intensity is large, while wave packets created by an unstable electron plasma wave (hybrid wave) during the beam-plasma interactions are also observed. The frequency of the plasma wave spreads over the width of 20 MHz and the center frequency is 432 MHz. By an analysis of the dispersion relation, the plasma wave is found to be a backward wave.

The physical process for generating the upper hybrid solitons from the ion waves is nonlinear Landau damping which is a nonlinear interaction between an ion wave and two upper hybrid waves. The electron plasma wave contributes as an original source of the ion wave as well as a source of electron heating by scattering.<sup>6</sup> Figure 4 shows the spatial distribution of the 0.1-MHz component of an ion wave and that of the upper hybrid waves; their frequencies are 399 and 432 MHz, respectively. The

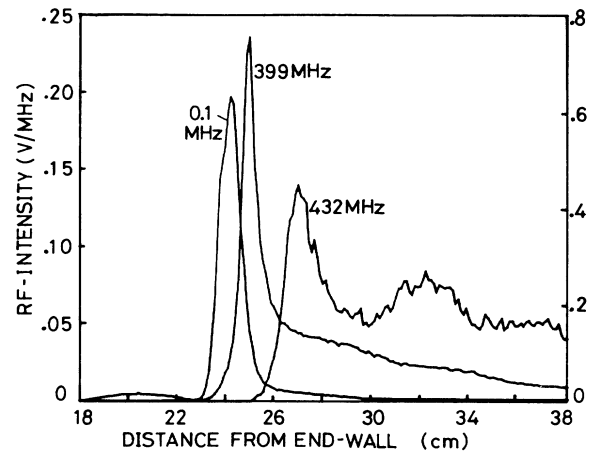


FIG. 4. Spatial distribution of 0.1-MHz component of the ion shock wave and that of the 399- and 432-MHz components of an upper hybrid wave. The scale on the right-hand side should be used for the 0.1-MHz wave.

scale of the right-hand side should be applied for the 0.1-MHz component and the scale of the left-hand side is used for other frequency components. The power spectrum of these signals are represented in units of volts per megahertz, where we assumed that the signal is impulse noise and not random noise.<sup>11</sup> An exponential growth of the 399-MHz component is accompanied by a damping of the 0.1-MHz component of an ion wave. The amplitude of the ion wave (shock wave) is lessened by the consumption of its energy through an energy-transfer process to the high-frequency wave.

Let us consider the spatial growth rate of the 399-MHz component in Fig. 4. We assume that an intensity,  $I$ , of rf (399 MHz) increases exponentially as  $I = I_0 \exp(\gamma'x)$ , where  $\gamma'$  represents the spatial growth rate and  $x$  is a distance. Figure 5 shows a semilogarithmic

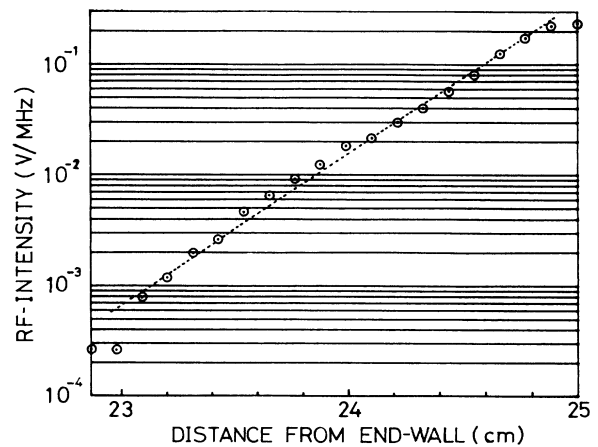


FIG. 5. Semilogarithmic plot of the rf intensity of the 399-MHz wave. From this exponential characteristic, we can obtain the value of spatial growth rate  $\gamma' = 310 \text{ m}^{-1}$ .

rithmic plot of the intensity. From the gradient of the straight line, we can get the spatial growth rate as  $\gamma' = 310 \text{ m}^{-1}$ . If the group velocity,  $U$ , of the rf is found, a time-growth rate,  $\gamma$ , can be obtained by the following relation:  $\gamma = U\gamma'$ .

The time-growth rates are obtained with two different methods. One is to get the group velocity,  $U$ , by a time-of-flight method and the other is obtained by a direct measurement of exponential rise time from an oscilloscope trace in Fig. 3.

The traveling time between two antennae which are 8 cm apart is  $8 \mu\text{s}$ . The group velocity of the upper hybrid wave,  $U$ , is therefore  $U = 10^4 \text{ m/s}$ . By using a spatial growth rate  $\gamma' = 310 \text{ m}^{-1}$ , one can get the growth rate  $\gamma = 3.1 \times 10^6 \text{ s}^{-1}$ . Direct measurement discussed above gives the value of the growth rate of  $2.92 \times 10^6 \text{ s}^{-1}$ . These values of the growth rate satisfy a weak-coupling criterion which describes a condition of weak turbulent plasma,<sup>12</sup>  $\gamma/\omega = 10^{-3} \ll 1$ , where the upper-hybrid-wave frequency of 399 MHz is used for  $\omega$ .

<sup>1</sup>M. Nambu, J. Phys. Soc. Jpn. **49**, 2349 (1980).

<sup>2</sup>M. Nambu, Phys. Fluids **25**, 1196 (1982).

<sup>3</sup>S. Bujarbarua, S. N. Saruma, and M. Nambu, Phys. Rev. A **29**, 2171 (1984).

<sup>4</sup>S. Bujarbarua, M. Nambu, and H. Fujiyama, Phys. Rev. A **31**, 3783 (1984).

<sup>5</sup>M. Nambu, J. Phys. Soc. Jpn. **54**, 2361 (1985).

<sup>6</sup>I. Mori and K. Ohya, IEEE Trans. Plasma Sci. **14**, 261 (1986).

<sup>7</sup>I. Mori, Rev. Sci. Instrum. **57**, 566 (1986).

<sup>8</sup>A. Hasegawa, *Plasma Instabilities and Nonlinear Effects* (Pergamon, New York, 1975), p. 145.

<sup>9</sup>K. Ohya and I. Mori, J. Appl. Phys. (Japan) **19**, 1193 (1980).

<sup>10</sup>V. I. Karpman, in *Nonlinear Waves in Dispersive Media*, edited by V. I. Karpman, translated by F. Cap (Pergamon, New York, 1975), p. 63.

<sup>11</sup>"Spectrum analysis... Noise measurements," Hewlett-Packard Spectrum Analyzer series, Applications Note No. 150-4, January 1973 (unpublished).

<sup>12</sup>B. B. Kadomtsev, in *Plasma Turbulence*, edited by M. G. Rusbridge (Academic, New York, 1965), p. 31.

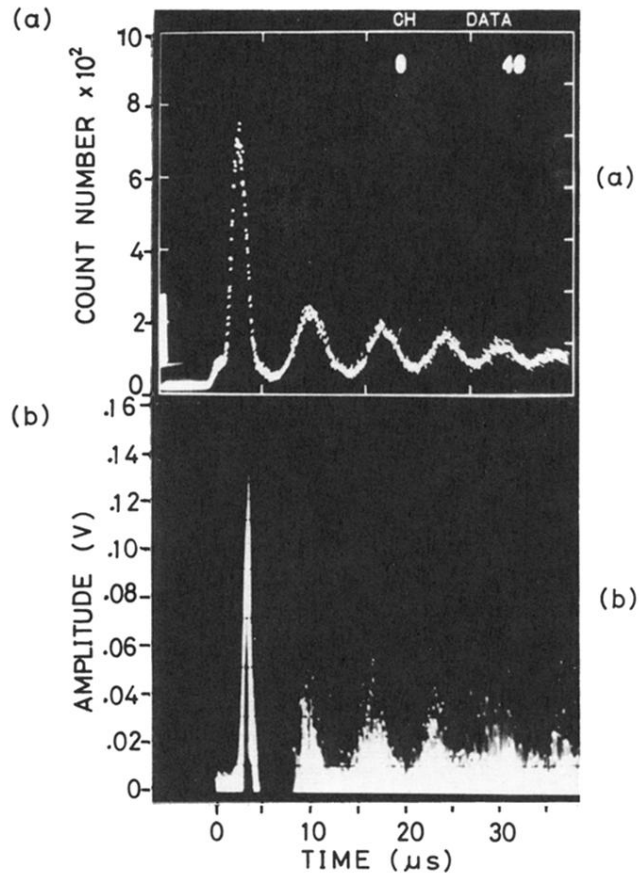


FIG. 2. (a) Profile of the ion shock wave obtained by the time-of-flight method. (b) High-frequency component of a collector current. The figure shows a high-frequency emission from the ion shock wave which is presented in (a).

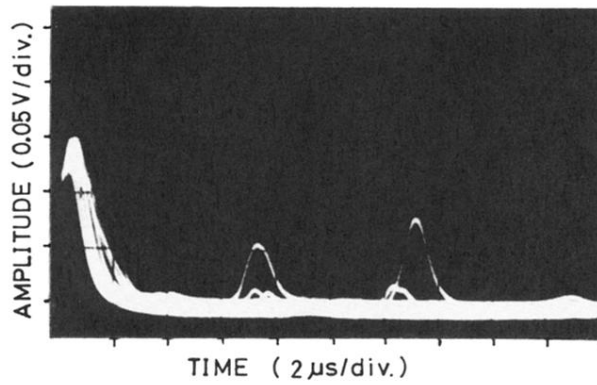


FIG. 3. Detected signal of high-frequency component in the collector current. The signal shows an envelope since it is detected by a diode.